

Structure of liquid tellurium: entangled, broken chains

This article has been downloaded from IOPscience. Please scroll down to see the full text article.

1990 J. Phys.: Condens. Matter 2 1271

(<http://iopscience.iop.org/0953-8984/2/5/018>)

View [the table of contents for this issue](#), or go to the [journal homepage](#) for more

Download details:

IP Address: 171.66.16.96

The article was downloaded on 10/05/2010 at 21:38

Please note that [terms and conditions apply](#).

Structure of liquid tellurium: entangled, broken chains

J Hafner

Theory of Condensed Matter Group, Cavendish Laboratory, University of Cambridge,
Madingley Road, Cambridge CB3 0HE, UK and
Institut für Theoretische Physik, Technische Universität Wien, Wiedner Hauptstrasse
8/10, A 1040 Wien, Austria†

Received 27 June 1989, in final form 10 October 1989

Abstract. We present a molecular-dynamics calculation of the structure of molten tellurium, based on effective interatomic forces derived from pseudopotential theory. Interatomic distances, coordination numbers, and bond angles are predicted in good agreement with recent neutron diffraction data. The analysis of the local topology shows that in liquid tellurium the atoms form a network of entangled broken chains with an average coordination number of $N_c = 2.5$ just above the melting point. We show that the physical mechanism stabilising this structure is the modulation of the random packing of the atoms in the melt by Friedel oscillations in the effective interatomic potential. We argue that this is just a generalised real-space description of the Peierls distortion argument conventionally used to explain the structure of crystalline Se and Te. The role of truly covalent interactions not included in this simple picture is discussed.

The purpose of this paper is to discuss the possibility of calculating the structure of liquid tellurium, starting from a very simple electronic theory of the interatomic forces.

It has long been recognised that liquid tellurium occupies a unique position halfway between semimetals and semiconductors: as pointed out by Enderby and co-workers [1, 2] the electrical resistivity, the Hall coefficient, the thermopower, and the Knight shift are beyond what can be explained straightforwardly using nearly-free-electron theory, but they are *just* beyond. With increasing temperature, liquid Te becomes distinctly more metallic. Cabane and Friedel [3] have shown that the number of free electrons per atom estimated from the Hall-effect and Knight-shift data increases from about one, just above the melting point ($T_M = 722.5$ K), to nearly three at $T \approx 1200$ K. Recent neutron scattering experiments [4, 5] have demonstrated that this change in the electronic properties is accompanied by an increase in the average coordination number from $N_c \approx 2.5$ at melting to $N_c \approx 3$ at $T \approx 1100$ K.

The structure of liquid Te is usually discussed with reference to its crystal structure. Crystalline Se and Te form a trigonal lattice, with helical chains of atoms running along the axes of the hexagonal cell. This structure may be considered as resulting from a

† Permanent address.

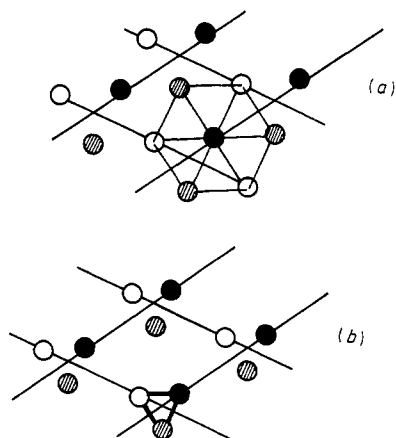


Figure 1. The structure of trigonal Se and Te. (a) Three close-packed layers stacked in an ABC sequence. (b) The trigonal structure projected onto the basis plane of the hexagonal cell. After [6].

distortion of close-packed layers stacked in an ABC sequence [6] (figure 1). Alternatively, the lattice may be derived from a simple cubic structure via a 'bond breaking' distortion. In the present context we shall find it more useful to relate the complex structure of either crystalline or liquid Te to a close-packed arrangement of atoms. While there is a general agreement that the structure of the liquid is similar to that of the crystal, the models proposed in the literature do differ as regards their details. Cabane and Friedel [3] have suggested that liquid Te consists of a random network of atoms that are either twofold or threefold coordinated. The fraction of tricoordinated sites increases with increasing temperature, and this should explain the more metallic behaviour. Pushing this idea further, Tsuchiya and Seymour [7] and Cutler and Rasolondramanitra [8] have developed an inhomogeneous structure model for liquid Te: it consists of two different domains; one has threefold coordination and is metallic, the other has twofold coordination and is semiconducting. On the other hand, Bellisent and Tourand [9, 10] have proposed a homogeneous model consisting of nearly freely rotating chains: while bond-distances and bond-angles are very similar to their values in the crystalline phase, the dihedral angles describing the relative orientation of successive bonds along a chain are assumed to have a completely random distribution.

The electronic mechanism stabilising the chain structure of Se and Te is usually described as a Peierls distortion, within either a tight-binding or a pseudopotential formalism [11]. In the group VI elements there are four p electrons per atom and hence the one-dimensional p bands along the chains of a simple cubic lattice (which are assumed to be non-interacting) are $2/3$ filled. Thus the Peierls distortion will lead to a lattice periodicity of $3a$ (where a is the lattice parameter of the simple cubic lattice) and a reduction of the coordination from six to two. Note that the same argument applies to the half-filled p bands of the group V elements where the Peierls distortion leads to a period-doubling and a threefold coordination. Very recently, Gaspard *et al* [12] have argued that lattice periodicity is not a necessary condition for the occurrence of a Peierls distortion, but that purely local considerations lead to the same result. Consequently, the conclusions can be applied to liquid and amorphous structures as well. The problem

is that if the Peierls argument correctly defines the conditions for a lattice instability to occur, it does not predict the actual magnitude of the distortion. This calculation requires further assumptions on the nature and strength of the repulsive interactions that held the atoms apart. In fact such a calculation is more easily performed in a real-space picture. Hafner and Heine [13] and Hafner and Kahl [14, 15] have discussed the trends in the crystalline and in the liquid structures of the s,p-bonded elements in terms of effective pair interactions derived from pseudopotential perturbation theory. The characteristic trends in the interatomic interactions with electron density and pseudopotential can be described in terms of two fundamental parameters: the effective radius R_c of the ionic core, and the electron-density parameter R_s (R_s is the radius of a sphere containing on the average one electron). The interatomic potential $\Phi(R)$ is repulsive at short distances, with the diameter of the repulsive core being given by [13, 16]

$$D_{\text{rep}} = 2R_c + 2\lambda_{\text{TF}} = 2R_c + 2 \times 0.456 R_s^{1/2} \quad (1)$$

where $\lambda_{\text{TF}} = 0.456 R_s^{1/2}$ is the Thomas–Fermi screening length. At intermediate and long distances, the potential $\Phi(R)$ is oscillatory, the wavelength of the oscillations being set by the Friedel wavelength λ_F :

$$\lambda_F = 2\pi/2k_F = 1.637 R_s. \quad (2)$$

It is the interplay of the repulsive and the oscillatory parts of the pair interaction, and between the pair and volume contributions to the total energy [13–16] that determines the trend in the atomic structures. At low electron densities, the position of the nearest-neighbour distance in a close-packed structure agrees with the position of the first attractive minimum in $\Phi(R)$. This explains the stability of highly coordinated metallic structures in groups I to III. As the electron density increases (R_s decreases), the repulsive core moves the first attractive minimum in $\Phi(R)$; see equations (1) and (2). If the close-packing distance coincides with a repulsive hump of $\Phi(R)$, then it will eventually be energetically favourable to split the first coordination shell into two subshells centred at

$$D_{1,2} = D_{\text{CP}} \pm \lambda_F/2. \quad (3)$$

(If $D_1 < D_{\text{rep}}$, then the largest possible distortion will be limited by the repulsive interactions.) Detailed molecular-dynamics simulations of liquid Si, Ge [17], and As [18] have shown that this mechanism of a modulation of the random close packing of the atoms by the Friedel oscillations in the effective interatomic interactions leads to a very accurate description of the liquid structures. Equation (3) may be regarded as a generalised real-space form of the Peierls distortion argument, although it does not refer to Brillouin zone and electron bands. In the conventional description of a Peierls distortion, the lowering of the total energy in the distorted structure results from the opening of an energy gap at the Fermi level. To first order, the width of the gap is given by $2|w(2k_F)|$. Note that it is precisely the same matrix element of the pseudopotential that sets the amplitude of the Friedel oscillations. The real-space form considerably extends the concept of a Peierls distortion and shows that the complex structures of the liquid group IV and V elements can be explained in terms of arguments [17–19] that apply to the crystalline and liquid structures of all the s,p-bonded elements from groups I to V.

Hence it is very tempting to extend these considerations to the group VI elements. In doing so we should remember that we are taking nearly-free-electron perturbation

theory to the very limits of its applicability. One point is that the dielectric function is very different in a metal and in a semiconductor. However the difference is mainly at long wavelength and affects the volume-dependent contributions to the total energy more than the effective interatomic pair potential. The structural energy differences and the effective pair interactions are determined mainly by the values of the pseudopotential at the first few reciprocal lattice vectors (or equivalently at the first peak in the static structure factor of the melt) and at these momentum transfers the screening functions of a metal and a semiconductor differ by less than ten per cent [11, 16]. The second point is that a proper description of true covalent bonding effects must include at least the leading higher (i.e. beyond second-order) corrections. It is well known that without these corrections, NFE perturbation theory predicts only the static stability of the diamond structure of Si and Ge relative to say a FCC structure, but not the dynamical stability of the diamond lattice itself. However, the calculations of the atomic and the electronic structures of the molten elements [17–19] have shown that these covalent corrections are minimised in the liquid phase. For this reason the liquids are an important reference phase for the dielectric theory of bonding.

Our calculation for liquid Te is based on the simplest possible approximation. We have used the empty-core pseudopotential [20] and the Ichimaru–Utsumi (IU) form of the local-field corrections to the dielectric function [21]. The IU screening function satisfies all the important sum rules for a response function, in particular the compressibility sum rule which is most important for obtaining the repulsive diameter of the ion correctly [22]. The core radius R_c has to be chosen such as to be in reasonable agreement with the known electronic properties of Te. In their analysis of empirical pseudopotentials, Cohen and Heine [23] show that for Te the first node of the empirical pseudopotentials fitted to the electronic properties occurs at $q_0/2k_F = 0.83$. This corresponds to a value of $R_c = 0.55 \text{ \AA}$ and this has been used in our calculation which has been performed at a fixed number density of $n = 0.0272 \text{ \AA}^{-3}$ and a temperature of $T = 723 \text{ K}$. The density has been taken from the data of Thurn and Ruska [24]. Note that the ratio $R_c/R_s = 0.48$ is very close to the value inferred from the structural trends [13, 15]. As explained in our previous paper [13] taking the density as given is essentially equivalent to modelling the non-locality of the pseudopotential by a second independent parameter.

The effective pair potential for liquid Te is shown in figure 2. It has the expected form with a strong inflection in the repulsive part. At the close-packing distance of $D_{CP} = 3.74 \text{ \AA}$ (calculated for FCC packing), both the radial and the tangential force constants are negative; hence a close-packed arrangement is clearly unstable. The distances D_1 , D_{CP} , and D_2 (calculated according to equation (3)) are in reasonable agreement with the interatomic distances in trigonal Te: d_1 the distance to two nearest neighbours inside a chain, d_2 the distance between an atom and its four nearest neighbours in the next chains, and d_3 the distance between neighbouring chains and between second neighbours in the same chain (altogether $6 + 2 = 8$ neighbours), cf. figure 1.

The structure of liquid Te has been calculated using classical microcanonical molecular dynamics (for details of our routines see [17, 18]) for ensembles with 216 to 1024 atoms in a cubic box. The oscillatory potential was cut off at a node at a distance corresponding to about 35 per cent of the edge of the cubic cell (for the largest cell this corresponds to $R_{cut} = 11.7 \text{ \AA}$, cf. figure 2). Although the core radius adjusted to the empirical pseudopotentials leads to very reasonable results for the liquid structure, the calculation was repeated for core radii ranging between $R_c = 0.52 \text{ \AA}$ and $R_c = 0.59 \text{ \AA}$. It was found that the results (in particular the interatomic distances and coordination numbers) are stable with respect to such variations in the pseudopotential.

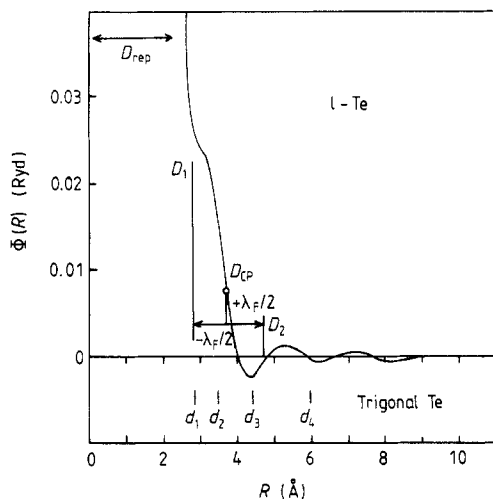


Figure 2. The effective pair potential $\Phi(R)$ for liquid Te. The nearest-neighbour distance D_{CP} in a close-packed structure is marked by a circle; the vertical bars mark the electronically driven distortion. The interatomic distances d_i in the trigonal lattice are indicated. Cf. text.

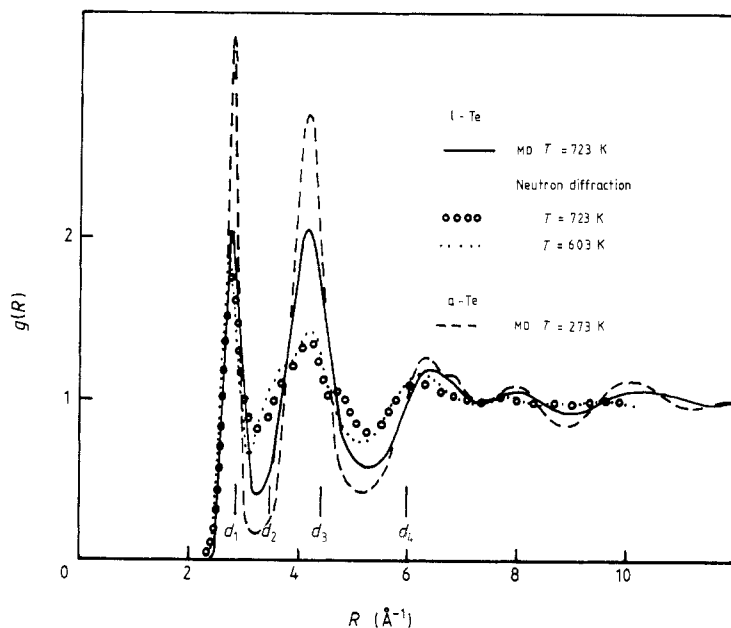


Figure 3. The molecular-dynamics results for the pair correlation function of liquid and amorphous Te, compared with the neutron diffraction data of Menelle *et al* [4, 5].

Figures 3 and 4 show the pair correlation function $g(R)$ and the static structure factor $S(q)$ at $T = 723$ K, and the corresponding neutron scattering data. Although a full quantitative agreement is certainly not to be expected, this very simple calculation reproduces the interatomic distances and coordination numbers surprisingly well: the first peak in $g(R)$ is situated at $R_1 = 2.76$ Å; the integration up to the first minimum ($R_{\min} = 3.2$ Å) yields a coordination number of $N_{c1} = 2.56$ (experimentally, $R_1 = 2.81$ Å, $N_{c1} = 2.63$ according to Menelle *et al* [4, 5]). The second peak occurs at $R_2 = 4.15$ Å

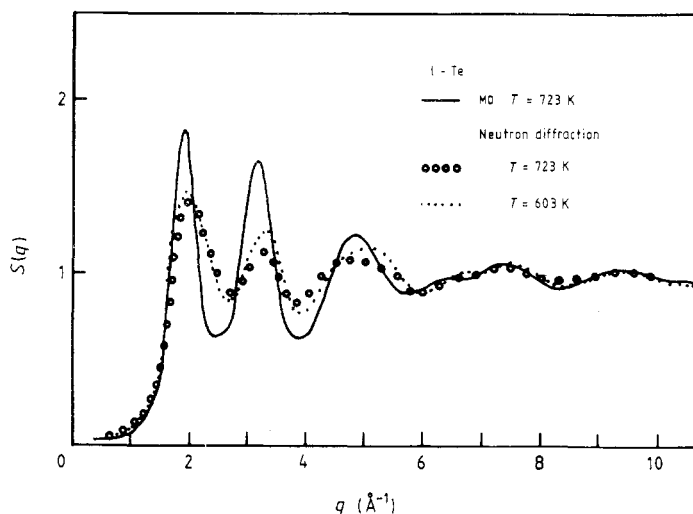


Figure 4. The static structure factor of liquid Te.

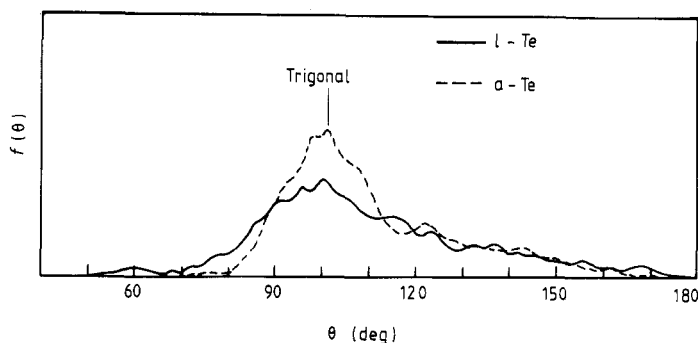


Figure 5. The bond-angle distribution function $f(\theta)$ in liquid and amorphous Te. The vertical bar marks the bond-angle in the crystalline structure.

(experimentally $R_2 = 4.20 \text{ \AA}$); integration of $g(R)$ from the first to the second minimum yields $N_{c2} = 14.48$, to be compared with the $2 + 4 + (6 + 2) = 14$ neighbours at these distances in trigonal Te (cf. above). The fact that we get the first- and second-nearest-neighbour distances right suggests that our model gives a correct description of the bond-angles: indeed figure 5 shows that the bond-angle distribution $f(\theta)$ has a single well defined peak at $\theta = 100^\circ$, i.e. very close to the bond angle of $\theta = 102^\circ$ in trigonal Te. The dihedral angles are randomly distributed (figure 6). All the characteristic details of the liquid structure are further enhanced if we quench the liquid to form a glassy phase (see figures 3 and 5). If the temperature is increased, the enhanced thermal disorder leads to a shallower minimum between the first and second peaks in $g(R)$ and hence to an increase in the coordination number towards $N_c \approx 3$, which has also been found in the neutron scattering experiments [4, 5].

To give a more direct impression of the structure of liquid Te, we show in figure 7 a projection of the atoms and nearest-neighbour bonds in an instantaneous configuration:

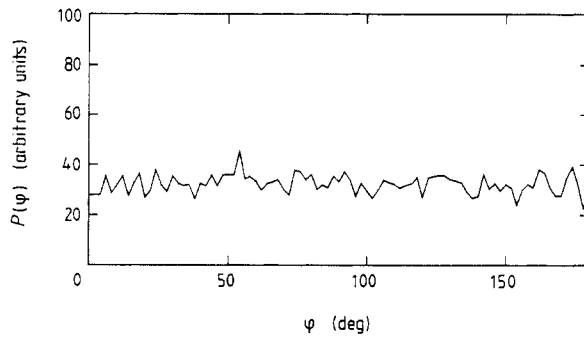


Figure 6. The distribution $P(\varphi)$ of the dihedral angles in liquid Te.

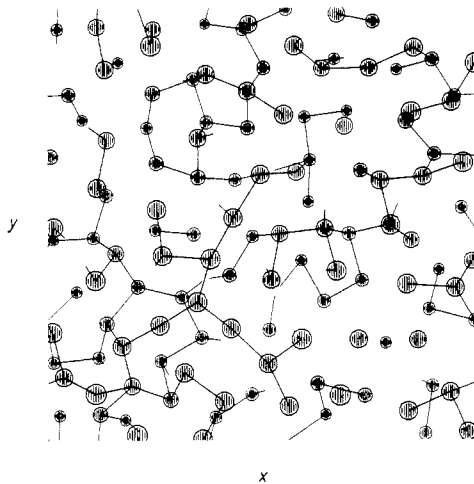


Figure 7. An instantaneous configuration of the atoms in liquid Te (cf. text). $T = 723$ K, $z_{\min} = 5.0$ Å, $z_{\max} = 11.4$ Å.

a slice of thickness $2R_{\min}$ (R_{\min} is a reasonable measure of the maximum bond length) is cut out of the MD cube. The atoms are projected on the xy -plane. The size of the symbols representing the atoms is scaled with the z -coordinate so that atoms close to the top of the layer appear larger. Nearest-neighbour bonds are drawn. If a bond connects to an atom outside the layer, the bond is cut at the surface. The picture shows clearly that *the atoms in liquid tellurium form entangled broken chains*. By following the time-evolution of such a configuration we find that these chains are continuously deformed and broken up, and the atoms recombine to form new chains. The lifetime of these chains can be estimated to be about 10^{-13} to 10^{-12} s.

Note that in this simple approach the local topology is entirely dominated by the form of the pair potential at short and intermediate distances: the comparison of figures 3 and 4 shows that there is a one-to-one correspondence between the peaks in $g(R)$ and the minima in $\Phi(R)$ which extends to about 10 Å. Hence the complex structure of liquid Te arises from the interplay of two characteristic distances: the effective size of the atom and the Friedel wavelength determined by the electron density. The important role of the electrons is also immediately evident from the static structure factor: the sharp second peak appears exactly at $q = 2k_F$. It is important to realise that it is the form of

the potential at distances corresponding to the first two or three coordination shells that is important, and not the long-range tail. This follows clearly from our simulations with different cut-off radii: the results shown here are essentially unchanged, even if the potential is cut off at the second node (i.e. at $R \approx 5.8 \text{ \AA}$).

The exceedingly simple approach we have presented here has two main shortcomings: (i) it ignores the very low electrical conductivity of liquid Te and hence the fact that the mean free path of the electrons is of the order of the interatomic distances, and (ii) the neglect of true covalent (i.e. angle-dependent interactions). The interplay of volume-forces and volume-dependent pair-forces includes covalency only in the sense of metallic interactions between overlapping spherical pseudoatoms, with no limit to the number of bonds an atom can form beyond the restrictions imposed by the packing requirements [16]. In the case of liquid Te we find that these constraints go a long way towards explaining the direction of a covalent bond: the mean interatomic distance imposed by the volume term and the form of the pair potential lead to the correct coordination number. The absence of 'true' covalency affects mainly the fluctuations in the local coordination which are certainly overestimated in our simple model.

It is relatively easy to correct for the finite mean free path of the electrons. It is well known that a finite mean free path leads to a smearing of the $2k_F$ -singularity in the free-electron response function and hence to a damping of the Friedel oscillations [25, 26]. Recent calculations on strong-scattering liquid alloys [26] have shown that even with a mean free path of the order of a few interatomic distances, the first two oscillations in the potential survive in a damped form, whereas the oscillatory tail is flattened. Hence we can expect that a proper inclusion of finite mean-free-path effects would reduce the height of the second-neighbour peak in $g(R)$ and even improve the agreement with experiment.

It is more difficult to assess the importance of angular interactions. The calculation of realistic many-body forces via the Hellmann-Feynman theorem involves computations that are several orders of magnitude more time consuming than the present calculations [27-29]. For liquid Si [27] and As [29] quantum-mechanical calculations of the liquid structure are now available. They tend to confirm the results obtained using perturbation theory [17, 18]. The covalent interactions in the liquid seem to be of a resonant character: bond charges and angular forces appear locally whenever the configuration is close to the ideal geometry [30]. At high temperatures these configurations are continuously formed and destroyed again; hence they have only a small influence on the structure of the liquid. At low temperatures, these energetically favourable configurations acquire a particular stability, and in Si and Ge this will eventually lead to a transition from a metallic liquid to a semiconducting glass. For liquid Te, a quantum-mechanical calculation of the liquid structure has now been started. Very preliminary results suggest that our simple picture is basically correct. The main effect of the many-body forces is a non-random distribution of the dihedral angles. This agrees with the observation made by Li and Allen that in liquid As the main differences between simulations based on volume- and pair-forces, and simulations using the full set of quantum-mechanical many-body forces are in the higher-order correlation functions. Our results of l-Te will be reported in due course [31].

To conclude: we have presented the first molecular-dynamics calculation of the structure of molten tellurium, based on interatomic forces derived from nearly-free electron perturbation theory. We find that the atoms in liquid Te form a network of short, entangled chains. We show that this structure results from the interplay of volume- and pair-forces and that the structure of liquid Te may be understood in terms of

arguments that explain the trends in the crystalline and liquid structures of all the s,p-bonded elements from groups I to VI in the Periodic Table.

Acknowledgments

I would like to thank Professor V Heine for stimulating discussions and for a critical reading of the manuscript. I thank Professor P B Allen for communicating the results of the density-functional molecular-dynamics simulation for l-As prior to publication. The hospitality of Clare College and the Cavendish Laboratory, Cambridge, where this paper has been written, is gratefully acknowledged. Financial support has been provided by the Royal Society and the Science and Engineering Research Council.

References

- [1] Enderby J E and Gay M 1980 *J. Non-Cryst. Solids* **35 + 36** 1269
- [2] Enderby J E and Barnes A C to be published
- [3] Cabane B and Friedel J 1971 *J. Physique* **32** 73
- [4] Menelle A, Bellissent R and Flank A M 1987 *Europhys. Lett.* **4** 705
- [5] Menelle A, Bellissent R and Flank A M 1989 *Physica* **156 + 157** 174
- [6] Pearson W B 1972 *The Physics and Chemistry of Metals and Alloys* (New York: Wiley) p 234
- [7] Tsuchiya Y and Seymour E F W 1985 *J. Phys. C: Solid State Phys.* **18** 4721
- [8] Cutler M and Rasolondramanitra H 1984 *J. Non-Cryst. Solids* **61 + 62** 1097
- [9] Bellissent R and Tourand G 1977 *Proc. 7th Int. Conf. Liquid and Amorphous Semiconductors (Edinburgh)* ed W Spear, p 98
- [10] Bellissent R and Tourand G 1980 *J. Non-Cryst. Solids* **35 + 36** 1221
- [11] Littlewood P B 1983 *Crit. Rev. Solid State Mater. Sci.* **11** 229
- [12] Gaspard J P, Marinelli F and Pellegatti A 1987 *Europhys. Lett.* **3** 1095
- [13] Hafner J and Heine V 1985 *J. Phys. F: Met. Phys.* **13** 2479
- [14] Hafner J and Kahl G 1984 *J. Phys. F: Met. Phys.* **14** 2259
- [15] Hafner J 1987 *From Hamiltonians to Phase Diagrams* (Berlin: Springer)
- [16] Heine V and Weaire D 1970 *Solid State Physics* vol 24 (New York: Academic) p 247
- [17] Arnold A, Mauser N and Hafner J 1989 *J. Phys.: Condens. Matter* **1** 965
- [18] Hafner J 1989 *Phys. Rev. Lett.* **62** 784
- [19] Jank W and Hafner J 1988 *Europhys. Lett.* **7** 623
- [20] Ashcroft N W 1966 *Phys. Lett.* **23** 48
- [21] Ichimaru S and Utsumi K 1981 *Phys. Rev. B* **24** 7385
- [22] Hafner J and Heine V 1986 *J. Phys. F: Met. Phys.* **16** 1429
- [23] Cohen M L and Heine V 1970 *Solid State Physics* vol 24 (New York: Academic) p 235
- [24] Thurn H and Ruska J 1971 *J. Non-Cryst. Solids* **22** 331
- [25] de Gennes P G 1982 *J. Physique* **23** 630
- [26] Hafner J 1989 *J. Phys.: Condens. Matter* **1** 1133
- [27] Car R and Parrinello M 1988 *Phys. Rev. Lett.* **60** 204
- [28] Payne M C, Joannopoulos J D, Allan D C, Teter M P and Vanderbilt D H 1986 *Phys. Rev. Lett.* **56** 2656
- [29] Li X P and Allen P W *Phys. Rev. Lett.* to be published
- [30] Stich I, Car R and Parrinello M 1989 *Phys. Rev. Lett.* **63** 2240
- [31] Hafner J and Payne M C to be published